Journal of The Electrochemical Society, **152** (9) A1804-A1814 (2005)
0013-4651/2005/152(9)/A1804/11/$7.00 © The Electrochemical Society, Inc.

Transport Phenomena in Polymer Electrolyte Membranes

I. Modeling Framework

J. Fimrite, H. Struchtrup, and N. Djilali[z]

Institute for Integrated Energy Systems, University of Victoria, Victoria, British Columbia, Canada V8W 3P6

This paper presents a critical examination and analysis of classical and recently proposed models for transport phenomena in polymer electrolyte membranes. Key experimental observations related to membrane conductivity, membrane hydration, and sorption isotherms are first reviewed. Proton transport mechanisms in bulk water, and the influence of the membrane phase on these mechanisms, are examined. Finally, various formulations and underlying assumptions to account for macroscopic transport are reviewed, and an analysis of the binary friction model (BFM) and dusty fluid model (DFM) is performed to resolve an outstanding formulation issue. It is shown that the BFM provides a physically consistent modeling framework and implicitly accounts for viscous transport (i.e., Schloegl equation), whereas the dusty fluid model erroneously accounts twice for viscous transport. In Part II we apply the BFM framework to develop a general transport model for perfluorosulfonic acid membranes.
 [DOI: 10.1149/1.1952627]

Manuscript submitted July 28, 2004; revised manuscript received March 18, 2005. Available electronically July 25, 2005.

Polymer electrolyte membrane fuel cells (PEMFCs) are an energy conversion technology that can be used in a wide range of power applications, from the subwatt to megawatt scale. PEMFCs use a solid polymer electrolyte, typically a perfluorosulfonic acid (PFSA) membrane as opposed to a liquid electrolyte or solid electrolyte, to electrically and mechanically isolate the anode and cathode while allowing for ion migration.[1,2] Nafion, manufactured by DuPont, is one of the most thoroughly used and studied membranes. Another family of membranes that holds some promise for use in PEMFCs is the group of sulfonated polyaromatic membranes, typically sulfonated polyetherketones. While research is being performed on other types of membranes, as well as hybrid membranes that might have even better-suited properties, information on these is scarce.[3-13]

The functionality of polymer electrolyte membranes depends on an array of coupled transport phenomena that determine water content and conductivity. The work presented here is motivated by the need to better understand these phenomena and to improve the way in which transport in membranes is modeled, particularly in the context of ongoing efforts to develop more comprehensive computational fuel cell model[14-18] that allow analysis and optimization of fuel cells in a design and development environment. Kreuer et al.[19] recently presented a comprehensive review of both microscopic and macroscopic modeling aspects of transport phenomena in PEMs. Microscopic modeling work for PEMs, including molecular dynamics simulations[20] and statistical mechanics modeling,[21-24] has focused primarily on Nafion membranes and has provided insight into some of the fundamental transport mechanisms. In the context of multidimensional fuel cell modeling, practical considerations dictate the use of macroscopic models.

The objective of this paper is to provide a critical examination of classical and recently proposed macroscopic models, and to determine a general framework suitable for modeling transport phenomena in polymer electrolyte membranes. Prior to examining the theoretical framework, we provide some brief background and a summary of key experimental observations related to membrane conductivity, membrane hydration, and sorption isotherms. We then examine the coupled transport mechanisms occurring within the "bulk" solvent. Of particular interest are the coupling and how the introduction of interactions with the membrane alters the transport mechanisms. By analyzing the binary friction and dusty fluid models, we elucidate some of the outstanding formulation issues, and finally show that the binary friction model provides a general and rational framework for modeling transport phenomena in polymer electrolyte membranes. In a follow-up paper,[25] we apply this modeling framework to develop a general binary friction membrane model (BFM2) that accounts for transport of proton and water in PFSA membranes, and we derive a new conductivity model termed the binary friction conductivity model (BCFM) for 1100 EW Nafion membrane, which we then use to estimate the model parameters.

[z] E-mail: ndjilali@uvic.ca

Background

Transport of protons and water are the two phenomena of prime interest, and prior to examining the mechanisms that govern their transport, it is useful to briefly review some of the background that informs model formulation, including relevant aspects of membrane morphology, hydration behavior, and sorption isotherms.

Membrane families.— Sulfonated fluoropolymer membranes (also referred to as perfluorinated ion exchange membranes) or perfluorosulfonic acid membranes (PFSAs) such as Nafion, are currently the membranes of choice in low-temperature fuel cells as they exhibit high conductivity (when adequately hydrated), good stability (both mechanical and chemical) within the operating environment of the fuel cell, and high permselectivity for nonionized molecules to limit crossover of reactants.[26] Sulfonated fluoropolymer membranes start with a polytetrafluoroethylene (PTFE) backbone that is sulfonated by adding a side chain ending in a sulfonic acid group ($-SO_3H$) to the PTFE backbone. The resulting macromolecule contains both hydrophobic and hydrophilic regions. Altering the length of the chains, and location of the side chain on the backbone, alters the equivalent weights of sulfonated fluoropolymer membranes. The equivalent weight (EW) and its inverse, the ion exchange capacity (IEC), are defined as

$$\mathrm{EW} = \frac{1}{\mathrm{IEC}} = \frac{\text{Weight of dry polymer sample in grams}}{\text{Number of moles of acid groups}} \quad [1]$$

There is a general consensus that a hydrated Nafion membrane forms a two-phase system consisting of a water-ion phase distributed throughout a partially crystallized perfluorinated matrix phase.[26-28] The crystallized portion of the membrane cross-links the polymer chains, preventing complete dissolution of the polymer at temperatures below the glass transition temperature of the polymer[26] ($\sim$405 K for Nafion[27]). For a detailed review and discussion of membrane morphology, readers are referred to Weber and Newman,[28] and to Kreuer et al.[19] Based on earlier work, Weber and Newman postulate the formation of approximately spherical clusters in regions with a high density of sulfonate heads, and an interfacial region that under vapor-equilibrated conditions consists of collapsed channels (Fig. 1) that can fill with water to form a liquid channel when the membrane is equilibrated with liquid water (Fig. 2). In their collapsed form, the channels allow for conductivity, since sorbed waters can dissociate from the sulfonate heads, but the

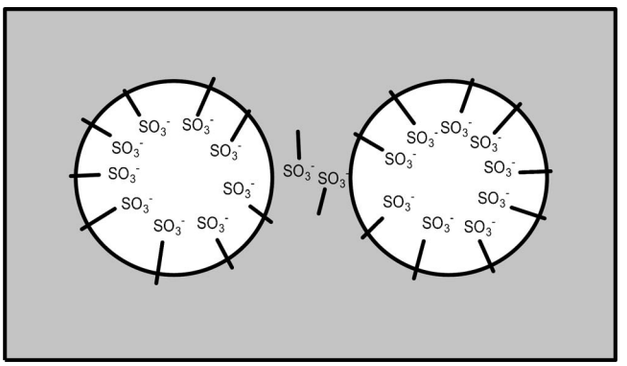

Figure 1. Schematic of vapor-equilibrated membrane showing the collapsed interconnecting channel, after Ref. 28.

amount of water sorbed is not sufficient to form a continuous liquid pathway.[28]

In addition to Nafion, the family of sulfonated fluoropolymers includes Dow chemical membranes and Membrane C. Weber and Newman predict that the clusters formed within Dow membranes are smaller than in Nafion due to the higher elastic deformation energy.[28] For sulfonated polyetherketone membranes, which are under investigation due to their potential in lowering costs, separation into hydrophobic and hydrophilic domains is not as well defined as in Nafion.[29] As a result, their structure consists of narrower channels and clusters that are not as well connected as in Nafion.[28,29]

Membrane hydration.— Modeling of water transport is important since the protonic conductivity is strongly dependent on the membrane water content. In order to understand the water transport and swelling behavior of PFSA membrane, we first examine the processes that take place as the membrane sorbs water molecules, focusing on Nafion, for which data for sorption of water is more readily available. It is anticipated that, due to similarities in morphology, other membranes would exhibit similar trends to those of Nafion.

Water sorption behavior of PEMs is commonly considered in terms of λ, the number of sorbed waters per sulfonate head. The anhydrous form ($\lambda = 0$) of the membrane is not common, since complete removal of water requires raising the temperature to a point where decomposition of the membrane begins to occur. Approximately one and a half waters per sulfonate head are considered to remain in a membrane that is not in contact with any vapor or liquid water.[27] The first waters sorbed cause the sulfonate heads to dissociate, resulting in the formation of hydronium ions.[27] The water that hydrates the membrane forms counterion clusters localized on sulfonate sites with the sulfonate heads acting as nucleation sites.[27]

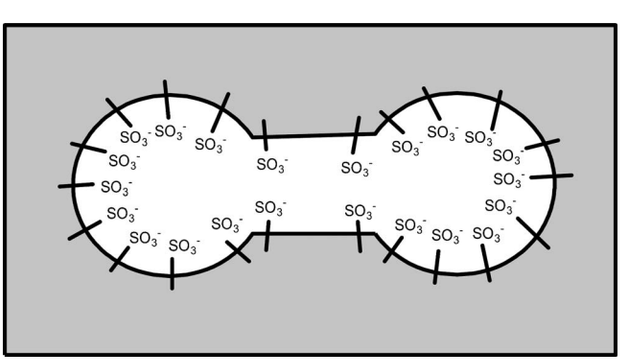

Figure 2. Schematic of liquid equilibrated membrane showing the interconnecting channel swollen, after Ref. 28.

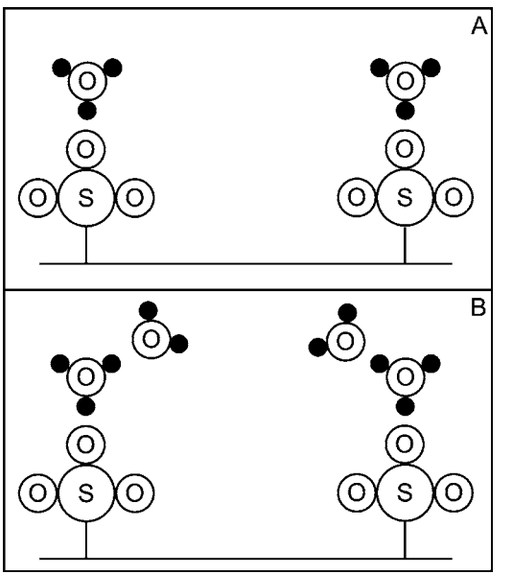

Figure 3. Schematic hydration diagram for Nafion for $\lambda = 1$ and $\lambda = 2$.

Given the hydrophobic nature of the backbone, and the hydrophilic nature of the sulfonate heads, it is reasonable to consider that all water molecules sorbed by the membrane at this low water content are associated with the sulfonate heads. Moreover, the hydronium ions will be localized on the sulfonate heads, and, because the amount of water sorbed is insufficient for the formation of a continuous water phase, the conductivity will be extremely low. Figure 3 is a schematic of the state of a membrane for λ in the range [1,2]. Note that the distance between sulfonate heads will be somewhat less in an actual membrane as sulfonate heads cluster together; thus, some transport is possible even at lower water contents ($\lambda \sim 2$).

For λ in the range [1,2], the hydrogen bonds have approximately 80% of the strength of those in pure water, but as more water is added to counterion clusters, the hydrogen bonds become weaker since the cluster shape does not allow for the formation of stronger bonds.[27] In the range $\lambda = [3\text{-}5]$, the counterion clusters continue to grow while the excess charge (proton) is mobile over the entire cluster.[27] For λ greater than 2, the membrane will conduct some protons as the excess protons are mobilized on the counterion clusters, and some pathways may be formed through the membrane to allow for conductivity. The membrane exhibits low conductivity for λ less than 5 (Fig. 4); as λ approaches 5, the membrane becomes more conductive as some counterion clusters may connect, but there is still insufficient water for all clusters to coalesce.[27]

Figure 5 shows the conductivity data of Sone et al.[30] for Nafion in the expanded form.[a] When λ drops from 5 to 2 (relative humidity drops from ~60 to ~13%) the conductivity decreases by about 2 orders of magnitude, whereas for λ between 5 and 14 (corresponding to relative humidity in the range of 60 to 100%) there is only a 1 order of magnitude variation. The extreme variation in conductivity in the range of $\lambda = [2,5]$ highlights how significant the formation of a continuous phase is.

Figure 6 illustrates the hydration state for $\lambda = [3,5]$. The number of water molecules forming the primary hydration shell for Nafion is expected to lie in the range [4,6].[32] Molecular dynamics simulations

[a]The *E* (expanded) form of Nafion has not been subjected to any heat treatment. The *N* (normal) form and the *S* (shrunken) form are heat treated at 80 and 105°C, respectively. The *N* form has some of the micropores joined and some closed compared to the *E* form, and the *S* form has even more pores closed compared to the *E* form (Ref. 30).

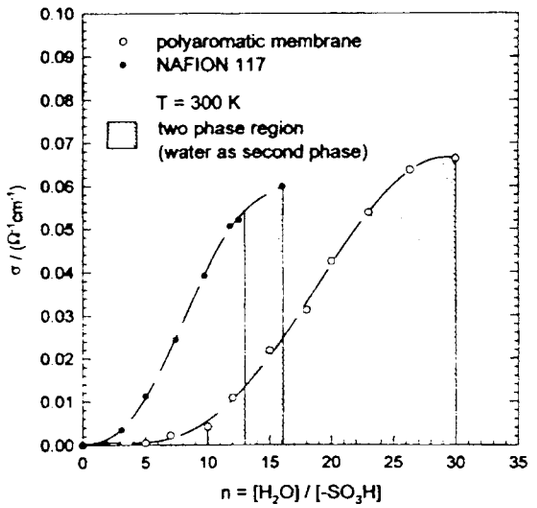

Figure 4. Room temperature proton conductivity of Nafion and a sulfonated polyaromatic membrane as a function of water content (Ref. 31).

indicate that 5 waters form the primary hydration shell for the sulfonate head, and any additional waters are not as strongly bound and thus form a free phase.[33,34]

For $\lambda \geqslant 6$, counterion clusters coalesce to form larger clusters, and eventually a continuous phase is formed with properties that approach those of bulk water.[27] This is supported by measurements that show that water mobility and water self-diffusion values approach the bulk water values;[35] the mobility of protonic charge carriers approaches the value in bulk water as well.[29] The free-water phase is screened (or shielded) from the sulfonate heads by the strongly bound water molecules of the primary hydration shell.[29,32] Figure 7 is a schematic representation of the hydration states for $\lambda = 6$ (near the conductivity threshold) and 14 (saturated vapor equilibrated).

Variations on this hydration scheme are expected for other PFSA membranes, as, among other factors, the number of waters in the primary hydration shell will vary according to the strength of the charge on the acid group, and the distance between sulfonate heads will affect the conductivity threshold, which will vary with the amount of water needed to connect the clusters.

Having described the hydration behavior, it is necessary to relate the equilibrium water content of the membrane λ to the activity of the solvent with which the membrane is equilibrated. This is done using experimentally determined sorption isotherms as shown in Fig. 8 for Nafion and a sulfonated polyaromatic membrane. The reliability of such sorption isotherms is critical for membrane transport models.[25] Both membranes in Fig. 8 exhibit the so-called Schroeder's paradox, an observed difference in the amount of water sorbed by a liquid-equilibrated membrane and a saturated vapor-equilibrated membrane, with both reservoirs at the same temperature

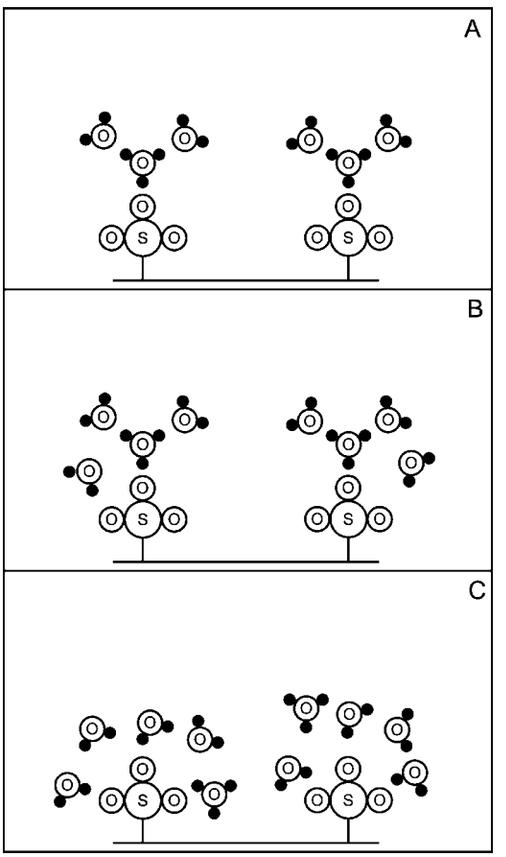

Figure 6. Schematic hydration diagram for Nafion for water contents of λ = 3-5.

and pressure.[28,36,37] This difference leads to the jump in lambda when the membrane is water equilibrated (activity = 1), as shown in Fig. 8. The best explanation for this phenomenon is probably that proposed by Choi and Datta,[32] who present a physicochemical model for water sorption which is consistent with the hydration scheme presented in the previous section. The water molecules sorbed by the membrane are assumed to be either strongly (chemically) bound to the sulfonate heads, or are "free" waters, which physically equilibrate with the external solvent. The number of chemically bound waters is determined by chemical equilibrium, while the number of free waters is determined by phase equilibrium.[32] Choi and Datta argue that an additional capillary pressure causes the vapor-equilibrated membrane to sorb less water than the liquid-equilibrated membrane from an external solvent with the same activity.

Choi and Datta's model and physically plausible explanation are

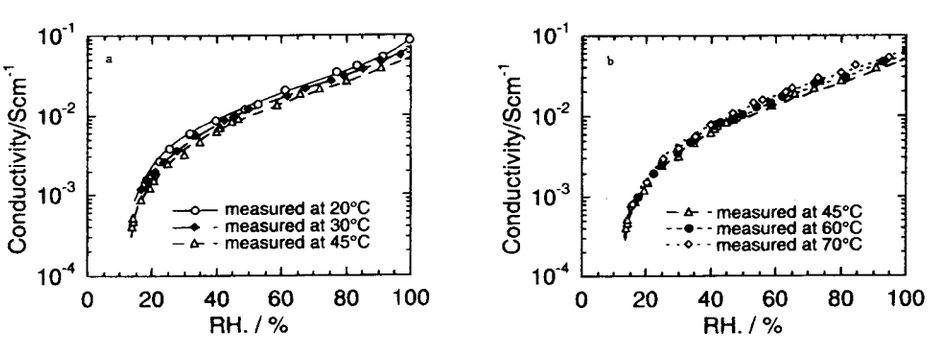

Figure 5. Conductivity dependence on temperature and relative humidity for the *E* form of Nafion (Ref. 30).

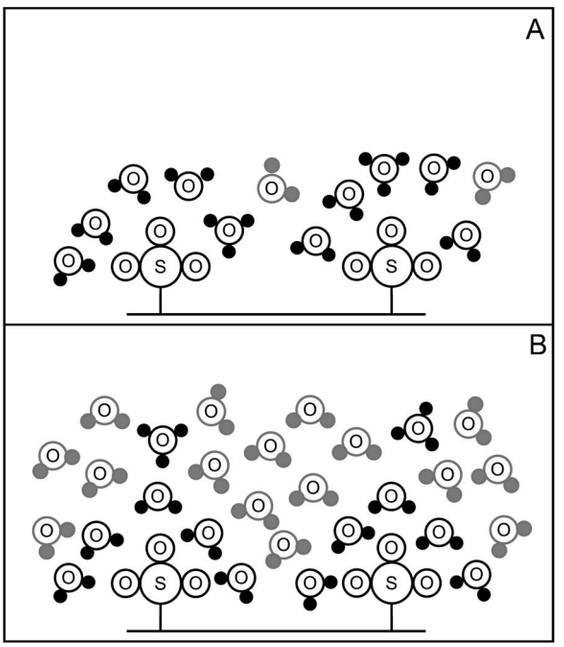

Figure 7. Hydration schematic for Nafion for λ = 6 and λ = 14. Free waters are shown in gray.

supported by good agreement with experimental data for vapor-equilibrated Nafion; see Fig. 9. The model also exhibits some generality. Assuming that the contact angle θ is approximately equal for Nafion and a sulfonated polyetherketone membrane, and considering the expression for the capillary pressure[33]

$$\Pi_\sigma = -\frac{2\sigma_w \cos\theta}{r_p} \quad [2]$$

we can explain the larger difference between the vapor-equilibrated and liquid-equilibrated uptake for the sulfonated polyetherketone membrane compared to Nafion (Fig. 8) with the smaller pore radius of the sulfonated polyetherketone membrane.

Transport mechanisms.— Having considered the sorption behavior of membranes, we now turn our focus to conductivity, a key performance parameter in fuel cells. In aqueous solutions (bulk water), the formation of protonic defects is suppressed by both the stability of the sp^3 hybrid (favoring ordered distribution of protons in space) and strong solvent effects.[38] However, the mobility of protonic defects in aqueous solutions is significantly higher than for other ions.[38,39] The high mobility of protons is afforded by the

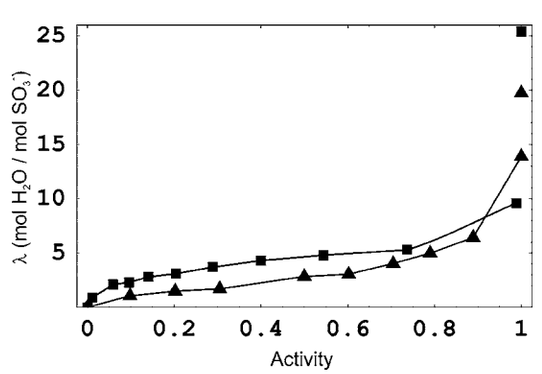

Figure 8. Water sorption isotherm for Nafion 117 (triangles) and a sulfonated polyaromatic membrane (squares) at 300 K (Ref. 31).

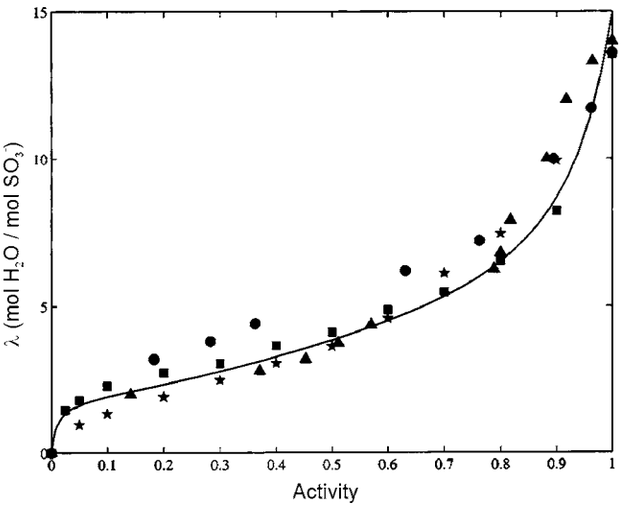

Figure 9. Water sorption isotherm for water vapor-equilibrated Nafion membrane (solid line is model prediction) (Ref. 32).

fact that the excess protons within the hydrogen bonded water network become indistinguishable from the "sea" of protons already present.[40]

Kreuer et al.[19] recently provided a state of the art review of proton transport mechanisms, and we will only briefly summarize relevant aspects. An excess proton in bulk water is typically found as a member of one of two structures, the first being a hydronium (H_3O^+) that is a proton donor to three other strongly bound waters.[38] The three strongly bound waters form the primary hydration shell of the hydronium, and the result is an "Eigen" ion[35,38,40] $(H_9O_4)^+$. The excess proton may also reside between two water molecules forming a "Zundel" ion[35,38,40] $(H_5O_2)^+$. The Zundel and Eigen ions are part of a fluctuating complex,[38] with the structure fluctuating between the Zundel and Eigen ions on a time scale of the order of 10^{-13} s.[35]

Proton diffusion can occur via two mechanisms, structural diffusion and vehicle diffusion.[38] It is the combination of these two diffusion mechanisms that confers protonic defects' exceptional conductivity in liquid water.

The conductivity of protons in aqueous systems of "bulk" water can be viewed as the limiting case for conductivity in PFSA membranes. When aqueous systems interact with the environment, such as in an acidic polymer membrane, the interaction reduces the conductivity of protons compared to that in bulk water.[38] In addition to the mechanisms described above, transport properties and conductivity of the aqueous phase of an acidic polymer membrane will also be effected by interactions with the sulfonate heads, and by restriction of the size of the aqueous phase that forms within acidic polymer membranes.[35] The effects of the introduction of the membrane can be considered on the molecular scale and on a longer-range scale; see Ref. 19 and 35. Of particular relevance to macroscopic models are the diffusion coefficients. As the amount of water sorbed by the membrane increases and the molecular scale effects are reduced, the properties approach those of bulk water on the molecular scale.[35] Figure 10 shows the trend in proton mobility D_σ and water self-diffusion D_{H_2O} for Nafion and a sulfonated polyetherketone membrane.

Another phenomenon linked to membrane conductivity is electro-osmotic drag, the process whereby a certain number of water molecules associated with a proton are dragged as the proton flows through the liquid phase of the membrane. The number of water molecules dragged through per proton is represented by the electro-osmotic drag coefficient ω_{pw}. Zawodzinski et al.[41] found that for a vapor-equilibrated membrane the electro-osmotic drag has a value of approximately 1 over a wide range of water vapor activities. For

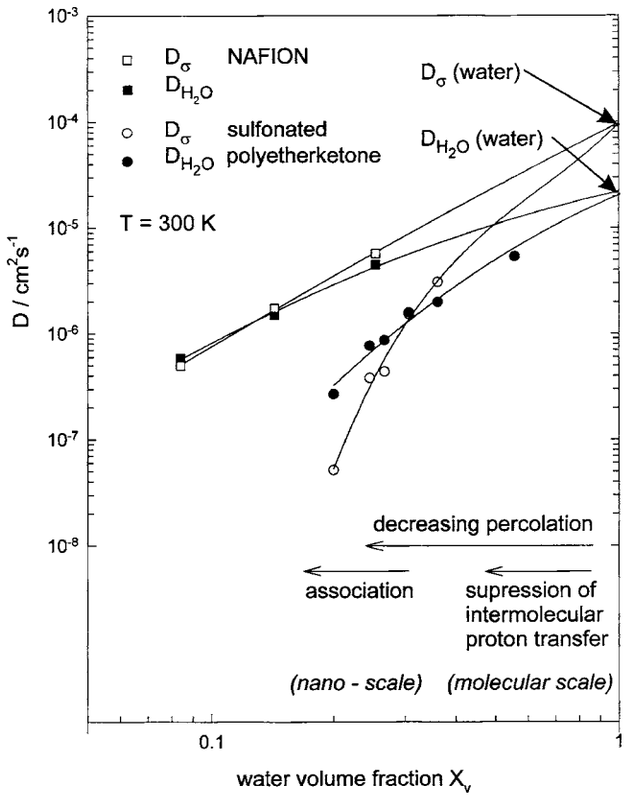

Figure 10. Proton conductivity diffusion coefficient D_σ and the molecular diffusion coefficient D_{H_2O} for two different polymers as a function of the water volume fraction. The values for pure water are given for comparison (Ref. 29).

a vapor-equilibrated membrane, within the collapsed channels (Fig. 1) there are only those waters present which strongly bind to the sulfonate heads, while the lower concentration of sulfonate heads means that this portion of the membrane is more hydrophobic than areas where clusters form. Thus, there is no free-water phase present in the collapsed channels. Consequently, we cannot expect large hydrated structures to diffuse through the membrane, as in bulk water. Instead, we expect the hydronium ions delocalized on the water molecules hydrating the sulfonate heads within the collapsed channels to allow for conductivity between clusters. Therefore, we have hydronium ions diffusing through the membrane liquid phase, which corresponds to an electro-osmotic drag coefficient of 1, as is expected for a vapor-equilibrated membrane.

Under liquid-equilibrated conditions (Fig. 2), the membrane liquid phase is well interconnected, and the effect of the sulfonate heads on the free water is reduced due to shielding; larger structures, such as Eigen and Zundel ions, can diffuse through the membrane liquid phase and, thus, more waters are dragged through the membrane per proton. Approximately 2.5 water molecules accompany each proton through the membrane for a liquid-equilibrated membrane.[28,42]

To simplify our modeling efforts, we assume that one water is carried through the membrane per proton over a wide range of water vapor activities, which is commonly done,[43,44] and approximately 2.5 water are carried through per proton when liquid-equilibrated.

Membrane Transport Models

In their recent review, Weber and Newman point out, "In terms of both quantitative and qualitative modeling, PEMs have been modeled within two extremes, the macroscopic and the microscopic."[28] The breadth of microscopic modeling work for PEMs

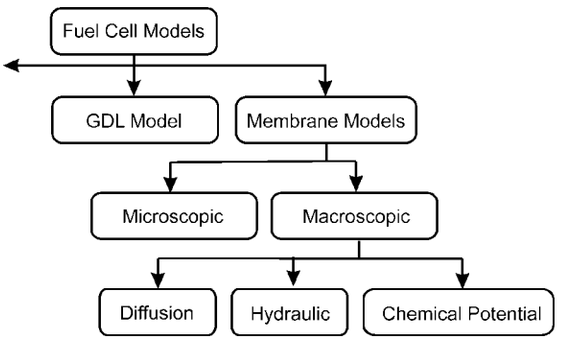

Figure 11. Classification of various modeling approaches.

encompasses molecular dynamics simulations[20] and statistical mechanics modeling.[21-24] Most applications have focused on Nafion, and interestingly, some models even apply macroscopic transport relations to the microscopic transport within a pore of a membrane.[45] Our focus is on macroscopic models required for computational simulations of complete fuel cells.[15,16]

Macroscopic models can be classified into two broad categories, as shown in Fig. 11: (*i*) membrane conductivity models, and (*ii*) models attempting to represent fuel cell processes, typically for water management purposes. The latter usually requires the use of a conductivity model, a fit to empirical data, or the assumption of constant conductivity (e.g., fully hydrated membrane at all times), and can be further classified into hydraulic models, in which a water transport is driven by a pressure gradient, and diffusion models, in which transport is driven by a gradient in water content.

Hydraulic models.— One of the earliest hydraulic models is that of Bernardi and Verbrugge[46,47] (see also Verbrugge and Hill[48,49]), which is based on the Nernst-Planck equation, including convection, for the transport of species within the fluid phase, and on the Schloegl equation to describe fluid transport

$$N_i^{N-P} = -z_i \frac{F}{RT} \mathsf{D}_i c_i \nabla \Phi - \mathsf{D}_i \nabla c_i + c_i v_s \qquad [3]$$

$$v_s = \frac{k_\Phi}{\eta} z_f c_f F \nabla \Phi - \frac{k_p}{\eta} \nabla p \qquad [4]$$

The theoretical basis of the Schloegl equation 4 will be revisited later. Bernardi and Verbrugge assumed a fully hydrated membrane, take the gases to be dissolved in the pore fluid, and because their focus is the cathode side of the fuel cell system, they only account for transport of oxygen through the membrane.[46] A more general variant of this hydraulic model was proposed by Eikerling et al.,[50] and allows water content variation, and dependence of conductivity, permeability, and electro-osmotic drag coefficient on the local water content.

The problem that arises when using hydraulic models is that, in membranes with lower water contents, interactions between the sulfonate heads and the backbone are significant, and the water molecules are localized on the sulfonate heads (see Fig. 3). The water is less "bulklike" and the clusters are no longer well connected. Conceptually, the concentration gradient seems to be a more appropriate driving force than the pressure gradient.[28]

Diffusion models.— The distinguishing feature of the classical diffusion models of Springer et al.[42] (hereafter SZG) is the consideration of variable conductivity. SZG relied on their own experimental data to determine model parameters, such as water sorption isotherms and membrane conductivity, as a function of the water content. Alternative approaches include the use of concentrated so-

lution theory to describe transport in the membrane,[51] and invoking simplifying assumptions such as thin membrane with uniform hydration.[52]

SZG's model has been particularly valuable in determining membrane resistance in computational fuel cell models for intermediate water content conditions. Such conditions are encountered in air breathing cells, but can also occur locally in humidified stacks. The SZG model has, however, several limitations. The conductivity is related to membrane water content and temperature by an empirical relationship. The equations used are not based on the physics of conductivity, but are essentially a curve fit and, thus, the model constants have no physical significance. Further, the model has very limited predictive capabilities and is restricted to 1100 EW Nafion. Even with parameter adjustments, SZG's model is not expected to be useful in predicting or correlating the behavior of other types of membranes.

Berg et al.[43] use the Nernst-Planck equation in their model; but, because they consider a concentration gradient as a driving force for the water flux, their model can be classified as a diffusion model. This is in contrast to Bernardi and Verbrugge, who use the so-called Schloegl equation, making their model a hydraulic model.

One of the problems with diffusion models is that, under conditions close to full hydration (Fig. 7b), there is essentially no water concentration gradient, and diffusion models are unable to produce a water concentration profile. In such regimes, a hydraulic model is more appropriate. Hence, diffusion models represent correctly the behavior at low water contents, while hydraulic models represent better the behavior in saturated membranes.[28]

An approach that is conceptually simpler and does not require the prescription of transport to hydraulic or diffusion mechanisms was proposed by Janssen,[53] and Thampan et al.[44] (hereafter TMT) based on the use of chemical potential gradients in the membrane. More recently, Weber and Newman[28] developed a novel model where the driving force for vapor-equilibrated membranes is the chemical potential gradient, and for liquid-equilibrated membranes it is the hydraulic pressure gradient. A continuous transition is assumed between vapor- and liquid-equilibrated regimes with corresponding transition from 1 to 2.5 for the electro-osmotic drag coefficient.

Membrane Conductivity Models

The model of TMT is one of the few models that is solely targeted at predicting conductivity behavior of a membrane, and in contrast to the model of SZG, is based on physical rather than purely empirical considerations.[44] It is in this vein that they invoke the dusty fluid model (DFM) to model transport in the membrane. Before considering the model of TMT, we examine the background of the DFM and the binary friction model (BFM).

The binary friction model.— The BFM is developed in Ref. 54 by considering the free solution within the membrane pore structure (Fig. 1 and 2) and applying the Stefan-Maxwell equations[55] to the pore fluid mixture to arrive at

$$\frac{X_i}{RT}\tilde{\nabla}_{T,p}\mu_i + \frac{\phi_i}{c_t RT}\tilde{\nabla}p - \frac{\rho_i}{c_t RT}\tilde{\mathbf{F}}_i^m = \sum_{j=1}^{n}\frac{(X_i\tilde{\mathbf{N}}_j' - X_j\tilde{\mathbf{N}}_i')}{c_t D_{ij}^{S-M}} \quad [5]$$

In the above equation the electrochemical potential has already been expanded to show explicitly the pressure and the external body forces $\tilde{\mathbf{F}}_i^m$. We start with this form, as it is the one used in the development of the BFM; however, we reintroduce later the electrochemical potential to allow comparison to other models.

The next steps in the derivation of the BFM are to assume that local equations apply to pore-averaged values (denoted with arrows) and to introduce the friction with the membrane (which is fixed and thus has zero velocity); thus[56]

$$\frac{1}{c_t RT}(c_i\vec{\nabla}_{T,p}\mu_i + \phi_i\vec{\nabla}p - \rho_i\vec{\mathbf{F}}_i^m) = \sum_{j=1}^{n} R_{ij}(X_i\vec{\mathbf{N}}_j - X_j\vec{\mathbf{N}}_i) - r_{iM}\vec{\mathbf{N}}_i \quad [6]$$

where $X_i = c_i/c_t$ was invoked with $c_t = \Sigma c_i$ as the total mole density of the fluid (refer to Ref. 56 for details). The resistance between species i and species j is

$$R_{ij} = \frac{1}{c_t D_{ij}^{S-M}} \quad [7]$$

while the resistance between species i and the membrane has been added in Eq. 6, and is defined as

$$r_{iM} = \frac{X_M}{c_t D_{iM}} = \frac{1}{c_t D_{iM}^e} \quad [8]$$

We note that D_{iM}^e is not a diffusion coefficient, but rather a membrane interaction term equivalent to an inverse friction coefficient between species i and the membrane.

Inserting Eq. 7 and 8 into Eq. 6 yields, after dropping the arrows to simplify the notation

$$\frac{-1}{c_i RT}(c_i\nabla_{T,p}\mu_i + \phi_i\nabla p - \rho_j\mathbf{F}_i^m) = \sum_{j=1}^{n}\frac{X_j}{D_{ij}^{S-M}}\left(\frac{\mathbf{N}_i'}{c_i} - \frac{\mathbf{N}_j'}{c_j}\right) + \frac{1}{c_i D_{iM}^e}\mathbf{N}_i' \quad [9]$$

Using the relation to convert an external force per unit mass of species i to an external force per mole of species i

$$\frac{\rho_i}{c_i}\mathbf{F}_i^m = \mathbf{F}_i \quad [10]$$

Considering the driving force, we know that[56]

$$\nabla_{T,p}\mu_i + \frac{\phi_i}{c_i}\nabla p - \mathbf{F}_i = \nabla_{T,p}\mu_i + \bar{V}_i\nabla p - \mathbf{F}_i = \nabla_T\mu_i - \mathbf{F}_i \quad [11]$$

and, because the only external forces acting on the charged ions are due to the gradient in potential, the driving force is the electrochemical potential gradient

$$\nabla_T\mu_i^e = \nabla_T\mu_i + z_i F\nabla\Phi \quad [12]$$

where z_i is the charge number of species i, F is Faraday's constant, and Φ is the electric potential in volts. Equation 11 becomes

$$\nabla_{T,p}\mu_i + \frac{\phi_i}{c_i}\nabla p - \mathbf{F}_i = \nabla_T\mu_i^e = \nabla_T\mu_i + z_i F\nabla\Phi \quad [13]$$

Substituting Eq. 12 back into Eq. 9 yields

$$\frac{-1}{RT}\nabla_T\mu_i^e = \sum_{j=1}^{n}\frac{X_j}{D_{ij}^{S-M}}\left(\frac{\mathbf{N}_i'}{c_i} - \frac{\mathbf{N}_j'}{c_j}\right) + \frac{1}{D_{iM}^e}\left(\frac{\mathbf{N}_i'}{c_i}\right) \quad [14]$$

There is yet another model referred to in the literature as a "diffusion" model.[57] This model is similar in nature to the BFM, but is derived by assuming the membrane can be modeled as a dust component (at rest) present in the fluid mixture. The equations governing species transport are developed from the Stefan-Maxwell equations with the membrane as one of the mixture species. The resulting equation for species i is identical to Eq. 14 above;[57] thus, the BFM and this diffusion model are equivalent.

In the BFM, as well as in the DFM and dusty gas model (DGM) discussed in detail in the next section, the structure of the porous media is considered independent of the transport equations. In the transport equations, the prime on the fluxes indicates that in fact these fluxes are the pore-averaged fluxes, and are taken per unit of *pore* surface area. We must correct these fluxes for the fact that

diffusion is occurring in a porous media with a given porosity ε and tortuosity factor[57] τ. The flux is corrected to a flux per unit of cross-sectional area of *membrane* nonprimed quantity by multiplying the primed flux by a correction factor that includes the porosity ε and tortuosity factor[55,56] τ

$$N_i = \frac{\varepsilon}{\tau} N_i' \quad [15]$$

The porosity and tortuosity factor can be brought into the diffusion coefficients[58]

$$D_{ij}^{\text{modified}} = \frac{\varepsilon}{\tau} D_{ij}^{\text{S–M}} \quad [16]$$

Thus, if we use the modified diffusion coefficients (Eq. 16), then the fluxes are considered to be defined on a membrane area basis and include porosity and tortuosity effects. One should note that it is not always desirable to bring the porosity and tortuosity correction into the diffusion coefficient terms, because this only complicates further their functional dependence on water content.

An alternative to the above correction is the Bruggeman correction[44]

$$D_{ij}^{\text{modified}} = (\varepsilon - \varepsilon_0)^q D_{ij}^{\text{S–M}} \quad [17]$$

where ε_0 is the threshold volume fraction, i.e., the minimum fraction of the volume that must be occupied by water before the water phase is sufficiently well connected to allow for transport. The Bruggeman exponent q is either used as a fitted parameter or is given the value of[44] 1.5. Note that for the appropriate q value the Bruggeman correction is equivalent to ε/τ.

The dusty fluid model.— In order to interpret the DFM and resolve the controversy that surrounds it, we must first examine the dusty gas model (DGM). The DGM was developed for gas flow through porous media, and is based on the premise that there are four independent mechanisms that drive gas transport through porous media. The first is Knudsen flow, where the gas pressure is low and collisions between the walls of the porous media and the molecules dominate; the second is viscous flow, in which molecule-molecule interactions dominate; the third is continuum diffusion, where molecule-molecule interactions dominate; and the fourth is surface diffusion, which is, however, neglected in the development of the model.[57]

The DGM equations for the total flux of a species can be derived from a Chapman-Enskog kinetic theory treatment, and, considering an isothermal system, this yields[b,57]

$$\sum_{j=1}^{v} \frac{c_j}{c_t D_{ij}^e}\left(\frac{\mathbf{N}_i'}{c_i} - \frac{\mathbf{N}_j'}{c_j}\right) + \frac{1}{D_{ik}^e}\left(\frac{\mathbf{N}_i'}{c_i}\right) + \frac{B_0}{D_{ik}^e \eta}\left(\nabla p - \sum_i c_i \mathbf{F}_i\right) = -\nabla \ln\left(\frac{c_i}{c_t}\right) - \nabla \ln p + \frac{\mathbf{F}_i}{k_B T} \quad [18]$$

Effective diffusion coefficients (superscript *e*) are introduced above, as the diffusion coefficients are not strictly Stefan-Maxwell diffusion coefficients, but rather have absorbed constants introduced by changing from considering the porous medium as part of the mixture to only considering the gas when calculating mole fractions.[58] The first term on the left of Eq. 18 accounts for continuum diffusion, the second for Knudsen diffusion, and the third for viscous flow. The primed flux variable $\mathbf{N}_i'$ denotes a pore-averaged flux relative to the rest frame of the porous medium.

[b]Note that we have elected to change the variables used by the original author from **J** to **N**, in light of the fact that these fluxes are molar fluxes relative to the rest frame of the porous medium, and to avoid confusion when comparing to other equations. In addition, we have also changed from molecular densities n to mole densities c so that the units of the fluxes remain consistent.

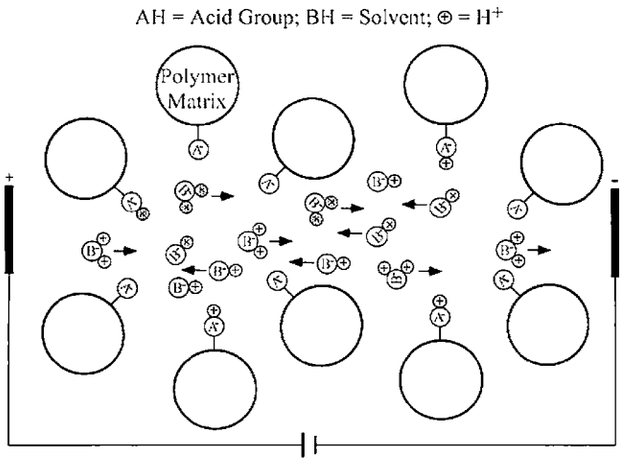

Figure 12. A "dusty-fluid model" depiction of a PEM. The polymer along with an acid group is viewed as "dust" particles, which comprise the PEM (Ref. 44).

In the dusty gas model, the total flux relative to the fixed reference frame is considered to consist of contributions from diffusion and convection, i.e., the total velocity of a species is made up of a diffusive contribution and a viscous flow (convective) contribution

$$\mathbf{N}_i' = c_i(\mathbf{v}_i^D + \mathbf{v}) \quad [19]$$

with

$$\mathbf{v} = -\frac{B_o}{\eta}(\nabla p - \sum_{i=1}^{v} c_i F_i) \quad [20]$$

The DGM was developed to model gas flow through porous media with high or low gas density and the transition regime in between the two ranges.[57] As a result of the different pressure dependencies of the various terms, different terms dominate in different regimes, thus allowing the model to predict behavior over a range of pressures.

The simplest derivation of the DFM involves arguments on the DGM. First, the driving forces (right side of Eq. 18) are converted to the chemical potential of the species within the pore liquid plus external body forces acting on that species. Second, the Knudsen diffusion term is now referred to as a membrane diffusion coefficient.[57] In the case of an isothermal system, with the only external body forces being the forces acting on the charged ions due to the gradient in potential, and substituting for the electrochemical potential Eq. 12, one obtains[57]

$$\frac{-1}{RT}\nabla_T \mu_i^e = \sum_{\substack{j=1 \\ j\neq i}}^{n} \frac{X_j}{D_{ij}^e}\left(\frac{\mathbf{N}_i'}{c_i} - \frac{\mathbf{N}_j'}{c_j}\right) + \frac{1}{D_{iM}^e}\left(\frac{\mathbf{N}_i'}{c_i}\right) + \frac{B_0}{\eta D_{iM}^e} \times \left[\nabla p + \left(\sum_{j=1}^{n} c_j z_j\right) F \nabla \Phi\right] \quad [21]$$

A second way to arrive at the above expressions was developed by Mason and Viehland, who started with the statistical mechanical work of Bearman and Kirkwood to arrive at Eq. 21.[56] Yet a third route is due to TMT, who introduced the membrane as a dust species in the mixture of diffusing species (Fig. 12). The membrane has zero velocity because it is mechanically restrained. The new mixture is modeled using the Stefan-Maxwell equations. The resulting equations are assumed to account for the diffusive velocity for a given species in the mixture that contains the membrane as a dust species (at rest).[44] It is then stated that the total species velocity is the sum of the diffusive and convective velocities $\{\mathbf{N}_i' = c_i\mathbf{v}_i = c_i(\mathbf{v}_i^D + \mathbf{v})\}$,

as the velocity in the Stefan-Maxwell equations does not account for viscous flow.[44] The convective velocity is given by the Schloegl equation[44]

$$\mathbf{v} = -\frac{B_0}{\eta}\left[\nabla p + \left(\sum_{j=1}^{n} c_j z_j\right) F \nabla \Phi\right] \quad [22]$$

The resulting transport equation, Eq. 10 in Ref. 44, can be divided by c_i to obtain Eq. 21.

Comparing the DFM and the BFM, we can clearly identify the extra terms in the dusty fluid model. It is these additional viscous terms which distinguish the DFM from the BFM. There are two schools of thought on the rationale for the additional terms. It is argued that the BFM (which is of a similar form as the Lightfoot model[56]) is correct and accounts for all interactions occurring between the membrane, and the species traveling through,[56,59] while proponents of the DFM argue that the model is correct by virtue of the additional viscous terms.[44,57,58]

One of the issues arising in the development of the DFM stems from the statement that the velocities in the Stefan-Maxwell equations are the diffusive velocities[44]

$$\frac{-c_i}{RT}\nabla_T \mu_i^e = \sum_{\substack{j=1 \\ j\neq i}}^{n} \frac{c_i c_j}{c_t D_{ij}^e}(\mathbf{v}_i^D - \mathbf{v}_j^D) + \frac{c_i}{D_{iM}^e}\mathbf{v}_i^D \quad [23]$$

and that a convective velocity must be added to the diffusive ones to yield velocities relative to the fixed reference frame (e.g., $\mathbf{v}_i = \mathbf{v}_i^D + \mathbf{v}$).

However, the relevant velocities in Eq. 23 are the *relative* velocities between the interacting species, so that the equation properly must be written as

$$\frac{-c_i}{RT}\nabla_T \mu_i^e = \sum_{\substack{j=1 \\ j\neq i}}^{n} \frac{c_i c_j}{c_t D_{ij}^e}(\mathbf{v}_i - \mathbf{v}_j) + \frac{c_i}{D_{iM}^e}(\mathbf{v}_i - \mathbf{v}_M) \quad [24]$$

where $\mathbf{v}_i$ and $\mathbf{v}_M$ are the velocities of species i and membrane M with respect to an *arbitrary* reference frame. Considering the rest frame of the membrane, where $\mathbf{v}_M = 0$, and introducing $\mathbf{v}_i = \mathbf{v}_i^D + \mathbf{v}$, where $\mathbf{v}$ is a mean velocity of the mixture moving against the membrane, leads to

$$\frac{-c_i}{RT}\nabla_T \mu_i^e = \sum_{\substack{j=1 \\ j\neq i}}^{n} \frac{c_i c_j}{c_t D_{ij}^e}(\mathbf{v}_i^D - \mathbf{v}_j^D) + \frac{c_i}{D_{iM}^e}\mathbf{v}_i \quad [25]$$

which is different from Eq. 23 in that it has the species velocity $\mathbf{v}_i$ (measured relative to the membrane) in the last term, and not the diffusion velocity $\mathbf{v}_i^D$. Note that the last equation is equivalent to Eq. 14, as can be seen when the relations between N, $\mathbf{v}$, c, and X are employed.

In addition, some proponents of the DFM have stated that the BFM does not account for viscous transport, and that an additional convective velocity, calculated using the Schloegl equation, must be added to the diffusive velocity. In the following section we will show that in fact the BFM model already contains the viscous terms, i.e., the Schloegl equation.

Schloegl equation and the BFM.— In order to demonstrate that the Schloegl equation is part of the BFM, we start by multiplying the BFM (Eq. 14) by X_i and substitute for ($\mathbf{N}_i' = c_i \mathbf{v}_i$), where $\mathbf{v}_i$ is the velocity of species i relative to the fixed reference frame (the membrane matrix), to yield

$$\frac{-X_i}{RT}\nabla_T \mu_i^e = \sum_j \frac{X_i X_j}{D_{ij}^{S-M}}(\mathbf{v}_i - \mathbf{v}_j) + \frac{X_i}{D_{iM}^e}\mathbf{v}_i \quad [26]$$

The velocity has diffusive and viscous contributions

$$\mathbf{v}_i = \mathbf{v}_i^D + \mathbf{v} \quad [27]$$

where mean velocity $\mathbf{v}$ and diffusive velocity $\mathbf{v}^D$ are defined so that

$$\mathbf{v} = \sum_i X_i \mathbf{v}_i \quad [28]$$

and

$$\sum_i X_i \mathbf{v}_i^D = 0 \quad [29]$$

Substituting Eq. 27 into 26, summing over all species i, and using Eq. 28 to simplify yields

$$\mathbf{v}\sum_i \frac{X_i}{D_{iM}^e} = -\frac{1}{RT}\sum_i X_i \nabla_T \mu_i^e - \sum_{i,j} \frac{X_i X_j}{D_{ij}^{S-M}}(\mathbf{v}_i^D - \mathbf{v}_j^D) - \sum_i \left(\frac{X_i}{D_{iM}^e}\mathbf{v}_i^D\right) \quad [30]$$

Due to the symmetry of D_{ij}^{S-M}, we have

$$\sum_{i,j} \frac{X_i X_j}{D_{ij}^{S-M}}(\mathbf{v}_i^D - \mathbf{v}_j^D) = \sum_{i,j} \frac{X_i X_j}{D_{ij}^{S-M}}\mathbf{v}_i^D - \sum_{i,j} \frac{X_i X_j}{D_{ij}^{S-M}}\mathbf{v}_j^D = \sum_{i,j} \frac{X_i X_j}{D_{ij}^{S-M}}\mathbf{v}_i^D - \sum_{i,j} \frac{X_i X_j}{D_{ji}^{S-M}}\mathbf{v}_i^D = 0 \quad [31]$$

Recall from Eq. 13 that the electrochemical potential gradient can be expanded into

$$\nabla_T \mu_i^e = \nabla_{T,p}\mu_i + \frac{\phi_i}{c_i}\nabla p + z_i F \nabla \Phi \quad [32]$$

and this gives for the first term on the right of Eq. 30

$$\sum_i X_i \nabla_T \mu_i^e = \sum_i X_i \nabla_{T,p}\mu_i + \frac{\sum_i \phi_i}{c_t}\nabla p + \sum_i z_i X_i F \nabla \Phi \quad [33]$$

where the sum of the volume fractions is equal to 1

$$\sum_i \phi_i = 1 \quad [34]$$

Combining Eq 30, 31, 33, and 34 yields

$$\mathbf{v}\sum_i \frac{X_i}{D_{iM}^e} = -\frac{\nabla p}{c_t RT} - \frac{F}{RT}\sum_i z_i X_i \nabla \Phi - \sum_i \left(\frac{X_i}{D_{iM}^e}\mathbf{v}_i^D\right) - \sum_i \frac{X_i}{RT}\nabla_{T,p}\mu_i \quad [35]$$

Assuming that we can neglect the activity coefficients, the chemical potential is[54]

$$\mu_i = g_i(T,p) + RT \ln X_i \quad [36]$$

so that

$$\frac{1}{RT}\nabla_{T,p}\mu_i = \frac{1}{X_i}\nabla_{T,p}X_i \quad [37]$$

Thus, we have

$$\sum_i \frac{X_i}{RT}\nabla_{T,p}\mu_i = \sum_i \nabla_{T,p}X_i = \nabla_{T,p}\sum_i X_i = 0 \quad [38]$$

Substituting Eq. 38 into Eq. 35, and rearranging, we finally obtain

$$\mathbf{v} = -\frac{1}{c_t RT}\frac{1}{\sum_i \frac{X_i}{D^e_{iM}}}\left(\nabla_p + F\sum_i z_i c_i \nabla \Phi\right) - \frac{\sum_i \left(\frac{X_i}{D^e_{iM}}\mathbf{v}_i^D\right)}{\sum_i \frac{X_i}{D^e_{iM}}} \quad [39]$$

We recall Eq. 29, and that the sum of the mole fractions is unity

$$\sum_i X_i = 1 \quad [40]$$

Therefore, assuming the membrane interaction terms are similar for all the species involved, we expect the last term in Eq. 39 to be small. Neglecting this last term in Eq. 39, we have

$$\mathbf{v} = -\frac{1}{c_t RT}\frac{1}{\sum_i \frac{X_i}{D^e_{iM}}}\left(\nabla_p + F\sum_i z_i c_i \nabla \Phi\right) \quad [41]$$

which is equivalent to the Schloegl equation (Eq. 22). The above argument demonstrates that the BFM equations do indeed account for the viscous transport, and that the addition of the viscous terms, as is done in the DFM, is not required.

Due to the ad hoc way in which the additional viscous terms are added into the fluid transport equations, the lack of rigorous justification for their addition, the incorrect statement that the velocities in the Stefan-Maxwell equations are diffusive velocities, and in light of the above proof that the viscous terms are included in the BFM, we have chosen to use the BFM as the modeling framework in our work.

Conductivity model based on the DFM.— Having considered the equations used to model transport in the membrane, we now turn our focus to an important stepping stone in theoretical modeling of conductivity, the model of TMT,[44] which is based on the DFM equations. Recalling the discussion on the Bruggeman correction, Eq. 17, TMT use this correction, with a percolation threshold below which conductivity is zero, in order to convert fluxes to a per unit cross-sectional area of membrane. In this way, TMT have accounted for the requirement of having a minimum amount of water sorbed by the membrane so that the water phase is sufficiently connected to allow charge conduction through the membrane. Although hydronium ion formation is the first step in the reaction of water molecules with a sulfonate head,[27] the hydronium is not necessarily free to move, but for lower water contents will instead be localized on the sulfonate head. Referring to Fig. 3b, we note that at such low water contents the liquid phase within the membrane is poorly connected.

The use of the Brunauer-Emmett-Teller (BET) sorption model by TMT is problematic because the BET is fit to sorption data at 30°C and the BET model does not consider the temperature dependence of sorption behavior. One way the model of TMT could be improved is by using more recent models of the sorption isotherms, e.g., that of Choi and Datta,[32] or by using conductivity data measured as a function of water content.

In developing the transport equations, TMT make several assumptions that should be re-examined in order to make further progress. Though it is probably reasonable to assume that hydronium ions are the charge carriers for vapor-equilibrated membranes, this is not valid for liquid-equilibrated membranes, where the transport number is found to be around[41] 2.5. For predictions in the liquid-equilibrated regime, as done by TMT, this assumption needs to be modified.

TMT assume equimolar counterdiffusion (closed conductivity cell), and thus the fluxes of water and hydronium are equal and opposite.[44] TMT acknowledge that the ratio of water and hydronium flux could be dictated by stoichiometry, or alternatively, a flux equation could also be written for water.[44] For a more complete transport model, it is desirable to develop a second flux expression for water, which considers the influence of forces (i.e., gradient in water molar density) that drive water through the membrane.

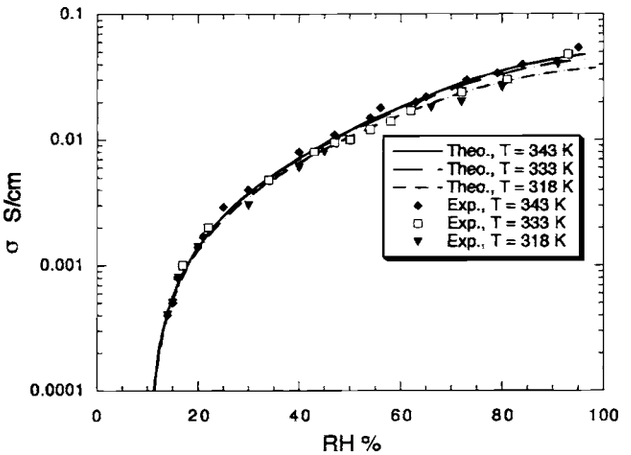

Figure 13. The experimental results of Sone et al. for σ of Nafion 117 equilibrated in water vapor vs RH or water vapor activity at different temperatures along with theoretical predictions of TMT (Ref. 44).

TMT also assume that[44] $D^e_{1M} \approx D^e_{2M}$. This needs to be reconsidered, because, due to the differences between the hydronium ions and water, we expect interaction forces with the membrane to be different for the different species. This assumption, coupled with the assumption of a closed conductivity cell, forces convection to be zero,[44] thus causing fortuitously the additional viscous terms to drop out anyway.

TMT's expression for conductivity in a closed conductivity cell is[44]

$$\sigma = (\varepsilon - \varepsilon_0)^q \left(\frac{\lambda_1^0}{1+\delta}\right) c_{HA,0}\alpha \quad [42]$$

where a complementary model was developed to represent the dissociation behavior, and thus allow determination of the fraction of dissociated acid groups α. In this model four empirically determined parameters are required. The BET model is fitted to sorption isotherms which yield C, the BET constant, and n_2, the total number of water layers sorbed on the pore surface. Two more parameters are required to fit the conductivity expression to conductivity data (Fig. 13): the percolation threshold volume fraction ε_0 and the ratio $D^e_{12}/D^e_{1M} = \delta$.

The conductivity expression, Eq. 42, provides a good visual fit to the experimental data of Sone et al.[30] for vapor-equilibrated membranes (Fig. 13), but the choice of a log-plot format to compare the model to experimental data can mask discrepancies. The model presented by TMT is significant in that it provides a theoretical framework based on the structure of the membrane and the physics of the transport. This modeling approach is not limited to Nafion, and should be applicable to other membranes with similar structures. However, there are several avenues for improvement:

1. The BFM can be used instead of the DFM, thus removing formulation inconsistencies due to the additional viscous terms. An interesting point is that TMT's assumption that $D^e_{1M} \approx D^e_{2M}$ actually causes the additional viscous terms to drop out anyway.
2. The restriction to equimolar counter diffusion could be removed.
3. The effect of temperature on the sorption isotherm could be accounted for.
4. Comparison should be done in a format where any differences between the model and experimental data can be more readily identified and estimated.

Conclusions

In Part I of this work we have presented a review of some relevant experimental and macroscopic modeling aspects of transport phenomena in polymer electrolyte membranes. This included examination of how the hydration scheme ties in with the behavior of the membrane, a plausible explanation of the so-called Schroeder's paradox, investigation of the proton transport mechanisms in bulk water, and the influence of the membrane phase on transport mechanisms. We also examined the various ways that different models have attempted to capture the transport phenomena occurring in the membrane. We have also resolved the controversy on the necessity of a viscous term in the membrane transport model, and shown that the binary friction model provides a physically consistent modeling framework. In the sequel to this paper, we develop a transport model for the polymer electrolyte membranes by applying the binary friction model, using the insight gained from this review and modeling framework analysis.

Acknowledgments

Dr. David Harrington and Dr. Brian Carnes provided very valuable insights and comments during the course of this work. This research was funded in part by grants to N.D. from the Natural Sciences and Engineering Research Council of Canada and the MITACS Network of Centres of Excellence.

University of Victoria assisted in meeting the publication costs of this article.

List of Symbols

a	activity of species i, 1
B_0	permeability, m^2
c	molar density of species i (Nernst-Planck equation), mol m^{-3}
D_i	diffusion coefficient (Nernst-Planck equation), m^2 s^{-1}
D_{ij}^e	effective concentration diffusion coefficient, m^2 s^{-1}
D_{ij}^{S-M}	Stefan-Maxwell diffusion coefficient, m^2 s^{-1}
D_{iK}^e	effective Knudsen diffusion coefficient, m^2 s^{-1}
D_{iM}^e	membrane diffusion coefficient, m^2 s^{-1}
EW	equivalent weight, g mol^{-1}
$\mathbf{F}$	external body force per mole, N mol^{-1}
IEC	ion exchange capacity, mol g^{-1}
k_ϕ	electrokinetic permeability (Nernst-Planck equation), m^2
k_p	hydraulic permeability (Nernst-Planck equation), m^2
$\mathbf{N}$	molar flux relative to fixed reference frame, mol m^{-2} s^{-1}
N_i^{N-P}	molar flux (Nernst-Planck equation), mol m^{-2} s^{-1}
n	molecular density (DGM equations), molecules m^{-3}
p	pressure, Pa
q	Bruggeman exponent, 1
R_{ij}	resistance between species i and j, m^2 s mol^{-1}
r_M	resistance between species i and the membrane, m^2 s mol^{-1}
r_p	average pore radius, m
T	temperature, K
$\mathbf{v}$	convective velocity, m s^{-1}
$\mathbf{v}_i$	average velocity of species i, m s^{-1}
v_S	velocity from Schloegl equation, m s^{-1}
X	mole fraction, 1
z	charge number, 1

Greek

α	degree of dissociation of acidic heads, 1
δ	ratio of mutual to membrane effective diffusion coefficients, 1
ε	porosity, 1
ε_0	threshold porosity, 1
η	viscosity, kg m^{-1} s^{-1}
θ	contact angle, 1
λ	number of waters sorbed per sulfonate head, 1
λ_i^0	equivalent conductance for species i at infinite dilution, S m^2 mol^{-1}
μ	chemical potential, J mol^{-1}
μ^e	electrochemical potential, J mol^{-1}
ρ	mass concentration, kg m^{-3}
σ	conductivity, S m^{-1}
σ_w	surface tension of water, N m^{-1}
τ	tortuosity factor, 1
Φ	potential, V
ϕ	volume fraction, 1
ω_{pw}	number of waters within hydrated proton complex, 1

Constants

R	universal gas constant 8.314 J mol^{-1} K^{-1}
F	Faraday's constant 96 485 C mol^{-1}
k_B	Boltzmann's constant 1.3807×10^{-23} J K^{-1}

Subscripts

i	species i
f	fixed species in membrane
l	protonated complex (typically hydronium ion)
2	waters participating in transport
pw	waters in protonated complex
sat	corresponding to saturated vapor conditions

Superscripts

o	standard state
e	effective
′	pore averaged flux per unit pore area
diff	diffusive
m	per unit mass

Abbreviations

SZG	Springer, Zawodzinski, and Gottesfeld (Ref. 42)
TMT	Thampan, Malhotra, Tang, and Datta (Ref. 44)

References

1. P. D. Beattie, F. P. Orfino, V. I. Basura, K. Zychowska, J. F. Ding, C. Chuy, J. Schmeisser, and S. Holdcroft. *J. Electroanal. Chem.*, **503**, 45 (2001).
2. J. Larminie, and Andrew Dicks, *Fuel Cell Systems Explained*, John Wiley & Sons Ltd, Ontario (2000).
3. C. Chuy, V. I. Basura, E. Simon, S. Holdcroft, J. Horsfall, and K. V. Lovell, *J. Electrochem. Soc.*, **147**, 4453 (2000).
4. J. Ding, C. Chuy, and S. Holdcroft, *Macromolecules*, **35**, 1348 (2002).
5. J. Ding, Q. Tang, and S. Holdcroft, *Aust. J. Chem.*, **55**, 461 (2002).
6. J, Kerres, A., Ullrich, T., Haring, M., Baldauf, U. Gebhardt, and W. Preidel, *J. New Mater. Electrochem. Syst.*, **3**, 229 (2000).
7. J. Kerres, W. Cui, R. Disson, and W. Neubrand, *J. Membr. Sci.*, **139**, 211 (1998).
8. C. Manea and M. Mulder, *J. Membr. Sci.*, **206**, 443 (2002).
9. M. K. Song, Y. T. Kim, J. M. Fenton, H. R. Kunz, and H. W. Rhee, *J. Power Sources*, **117**, 14 (2003).
10. V. I. Basura, C. Chuy, P. D. Beattie, and S. Holdcroft, *J. Electroanal. Chem.*, **501**, 77 (2001).
11. O. Savadogo, *J. New Mater. Electrochem. Syst.*, **1**, 47 (1998).
12. J. J. Sumner, S. E. Creager, J. J. Ma, and D. D. DesMarteau, *J. Electrochem. Soc.*, **145**, 107 (1998).
13. J. S. Wainright, J. T. Wang, D. Weng, R. F. Savinell, and M. Litt, *J. Electrochem. Soc.*, **142**, L121 (1995).
14. T. Berning and N. Djilali, *J. Electrochem. Soc.*, **150**, A1589 (2003).
15. S. Um and C. Y. Wang, *J. Power Sources*, **125**, 40 (2004).
16. P. T. Nguyen, T. Berning, and N. Djilali, *J. Power Sources*, **130**, 149 (2004).
17. A. Z. Weber and J. Newman, *Chem. Rev. (Washington, D.C.)*, **104**, 4679 (2004).
18. B. Sivertsen and N. Djilali, *J. Power Sources*, **141**, 65 (2005).
19. K. D. Kreuer, S. Paddison, E. Spohr, and M. Schuster, *Chem. Rev. (Washington, D.C.)*, **104**, 4637 (2004).
20. X. D. Din and E. E. Michaelides, *AIChE J.*, **44**, 35 (1998).
21. S. J. Paddison, R. Paul, and T. A. Zawodzinski, *J. Chem. Phys.*, **115**, 7753 (2001).
22. R. Paul and S. J. Paddison, *J. Chem. Phys.*, **115**, 7762 (2001).
23. S. J. Paddison, R. Paul, and T. A. Zawodzinski, *J. Electrochem. Soc.*, **147**, 617 (2000).
24. M. Eikerling, A. A. Kornyshev, and U. Stimming, *J. Phys. Chem. B*, **101**, 10807 (1997).
25. J. Fimrite, B. Carnes, H. Struchtrup, and N. Djilali, *J. Electrochem. Soc.* **152**, A1815 (2005).
26. G. Inzelt, M. Pineri, J. W. Schultze, and M. A. Vorotyntsev, *Electrochim. Acta*, **45**, 2403 (2000).
27. M. Laporta, M. Pegoraro, and I. Zanderighi, *Phys. Chem. Chem. Phys.*, **1**, 4619 (1999).
28. A. Z. Weber and J. Newman, *J. Electrochem. Soc.*, **150**, A1008 (2003).
29. K. D. Kreuer *J. Membr. Sci.*, **185**, 29 (2000).
30. Y. Sone, P. Ekdunge, and D. Simonsson, *J. Electrochem. Soc.*, **143**, 1254 (1996).
31. K. D. Kreuer, *Solid State Ionics*, **97**, 1 (1997).
32. P. Choi and R. Datta, *J. Electrochem. Soc.*, **150**, E601 (2003).
33. J. Elliot, S. Hanna, A. M. S. Elliot, and G. E. Cooley, *Phys. Chem. Chem. Phys.*, **1**, 4855 (1999).
34. A. Vishnyakov and A. V. Neimark, *J. Phys. Chem. B*, **104**, 4471 (2000).
35. K. D. Kreuer, *Solid State Ionics*, **136**, 149 (2000).
36. T. A. Zawodzinski, T. E. Springer, J. Davey, R. Jestel, C. Lopez, J. Valerio, and S. Gottesfeld, *J. Electrochem. Soc.*, **140**, 1981 (1993).
37. T. A. Zawodzinski, C. Derouin, S. Radzinski, R. J. Sherman, V. T. Smith, T. E.

Springer, and S. Gottesfeld, *J. Electrochem. Soc.*, **140**, 1041 (1993).
38. K. D. Kreuer, *Chem. Mater.*, **8**, 610 (1996).
39. N. Agmon, *Chem. Phys. Lett.*, **244**, 456 (1995).
40. M. Eikerling, A. A. Kornyshev, A. M. Kuznetsov, J. Ulstrop, and S. Walbran, *J. Phys. Chem. B*, **105**, 3646 (2001).
41. Z T. A. Zawodzinski, J. Davey, J. Valerio, and S. Gottesfeld, *Electrochim. Acta*, **40**, 297 (1995).
42. T. E. Springer, T. A. Zawodzinski, and S. Gottesfeld, *J. Electrochem. Soc.*, **138**, 2334 (1991).
43. P. Berg, K. Promislow, J. St-Pierre, J. Stumper, and B. Wetton, *J. Electrochem. Soc.*, **151**, A341 (2004).
44. T. Thampan, S. Malhotra, H. Tang, and R. Datta, *J. Electrochem. Soc.*, **147**, 3242 (2000).
45. B. R. Breslau and I. F. Miller, *Ind. Eng. Chem. Fundam.*, **10**, 554 (1971).
46. M. Verbrugge and D. Bernardi, *AIChE J.*, **37**, 1151 (1991).
47. M. Verbrugge and D. Bernardi, *J. Electrochem. Soc.*, **139**, 2477 (1992).
48. M. Verbrugge and R. F. Hill, *J. Electrochem. Soc.*, **137**, 1131 (1990).
49. M. Verbrugge and R. F. Hill, *J. Electrochem. Soc.*, **137**, 886 (1990).
50. M. Eikerling, Y. I. Kharkats, A. A. Kornyshev, and Y. M. Volfkovich, *J. Electrochem. Soc.*, **145**, 2684 (1998).
51. T. Fuller and J. Newman, *J. Electrochem. Soc.*, **140**, 1218 (1993).
52. D. M. Bernardi, *J. Electrochem. Soc.*, **137**, 3344 (1990).
53. G. J. M. Janssen, *J. Electrochem. Soc.*, **148**, A1313 (2001).
54. M. J. Moran and H. N. Shapiro, *Fundamentals of Engineering Thermodynamics*, John Wiley & Sons, New York (1996).
55. R. Taylor and R. Krishna, *Multicomponent Mass Transfer*, John Wiley & Sons, Toronto (1993).
56. P. J. A. M. Kerkhof, *Chem. Eng. J.*, **64**, 319 (1996).
57. E. A. Mason and A. P. Malinauskas, *Gas Transport in Porous Media; The Dusty Gas Model*, Elsevier, Amsterdam (1983).
58. R. Krishna and J. A. Wesselingh, *Chem. Eng. Sci.*, **52**, 861 (1997).
59. E. N. Lightfoot, *Transport Phenomena and Living Systems*, John Wiley & Sons, Toronto (1974).